

Lidocaine carboxymethylcellulose with gelatine co-polymer hydrogel delivery by combined microneedle and ultrasound

Atul Nayak, Hiten Babla, Tao Han, and Diganta Bhusan Das

Department of Chemical Engineering, Loughborough University, Loughborough, UK

Abstract

A study that combines microneedles (MNs) and sonophoresis pre-treatment was explored to determine their combined effects on percutaneous delivery of lidocaine from a polymeric hydrogel formulation. Varying ratios of carboxymethylcellulose and gelatine (NaCMC/gel ranges 1:1.60–1:2.66) loaded with lidocaine were prepared and characterized for zeta potential and particle size. Additionally, variations in the formulation drying techniques were explored during the formulation stage. *Ex vivo* permeation studies using Franz diffusion cells measured lidocaine permeation through porcine skin after pre-treatment with stainless steel MNs and 20 kHz sonophoresis for 5- and 10-min durations. A stable formulation was related to a lower gelatine mass ratio because of smaller mean particle sizes and high zeta potential. Lidocaine permeability in skin revealed some increases in permeability from combined MN and ultrasound pre-treatment studies. Furthermore, up to 4.8-fold increase in the combined application was observed compared with separate pre-treatments after 30 min. Sonophoresis pre-treatment alone showed insignificant enhancement in lidocaine permeation during the initial 2 h period. MN application increased permeability at a time of 0.5 h for up to ~17 fold with an average up to 4 fold. The time required to reach therapeutic levels of lidocaine was decreased to less than 7 min. Overall, the attempted approach promises to be a viable alternative to conventional lidocaine delivery methods involving painful injections by hypodermic needles. The mass transfer effects were fairly enhanced and the lowest amount of lidocaine in skin was 99.7% of the delivered amount at a time of 3 h for lidocaine NaCMC/GEL 1:2.66 after low-frequency sonophoresis and MN treatment.

Keywords

Carboxymethylcellulose, gelatine, lidocaine, microneedles, percutaneous delivery, sonophoresis

History

Received 25 April 2014
Revised 13 June 2014
Accepted 14 June 2014

Introduction

This paper is concerned with the delivery of lidocaine hydrochloride, a common anaesthetic, from a lidocaine carboxymethylcellulose with gel co-polymer hydrogel formulation such as discussed recently by Nayak et al. (2014). Lidocaine hydrochloride, termed as lidocaine from now on, is a water-soluble weak acid, fully ionized at pH 5.0 and administered into the plasma-rich layer under the skin surface (Igaki et al., 2013). However, this administration is conventionally performed via hypodermic needles as a low-cost and fast-acting method (Hedge et al., 2011; Kim et al., 2012). This is known to cause significant pains (Scarfone et al., 1998). Alternatives, such as eutectic mixture of local anaesthetics, topical lidocaine, require at least an hour of application to achieve effective analgesia, thus limiting its use especially in emergency situations (Nayak & Das, 2013). Therefore, there are important rationales for the pursuits of alternative lidocaine administration (Nayak & Das, 2013;

Nayak et al., 2014). This can be evidenced in the European paediatric drug legislation which backs innovation to develop “easy to administer” and “minimally invasive” drug delivery methods (Shah et al., 2011). The alternative rationales for lidocaine delivery include increased safety amongst the patients and healthcare providers, increased compliance with those who possess a fear of needles, reduced discomfort and pain especially in the case of applying anaesthetics as well as improved ease of delivery (Giudice & Campbell, 2006; Gill & Prausnitz, 2007; Li et al., 2010). Low bioavailability of some drugs limits the therapeutic target effect (De Boer et al., 1979; Huet & Leloir, 1980; Benet et al., 1996; Shipton, 2012). Lidocaine’s oral bioavailability is approximately reduced by 65–96% by digestive enzymes (Fen-Lin et al., 1993; Fasinu et al., 2011). In principle, innovative percutaneous delivery could overcome the barriers associated with direct injection and oral drug administration (Polat et al., 2011) such as lidocaine. The rate of passive diffusion (PD) of drugs by percutaneous delivery depends on the molecular structure, size and hydrophobicity in conjunction with the drug concentration gradients. However, many studies have used combinations of PD and non-invasive techniques with varying success, e.g. MNs and ultrasound (Chen et al., 2010; Han & Das, 2013). This is the topic of this paper and it is discussed in more detail below.

Address for correspondence: Diganta Bhusan Das, Department of Chemical Engineering, Loughborough University, Loughborough LE11 3TU, UK. Tel: 0044 1509 22509. Fax: 0044 1509 223923. E-mail: d.b.das@lboro.ac.uk

MNs are needle-like structures of the size order of microns commonly arranged in a matrix (Gill & Prausnitz, 2007; Olatunji et al., 2014; Zhang et al., in press). The lidocaine NaCMC/GEL hydrogels pseudo-plasticity property permits seepage into microneedle (MN) cavities to bypass the stratum corneum (SC) skin layer compared with passive diffusion (Nayak et al., 2014). Research has shown significant increases in skin permeability using optimized MNs when considering factors of MN length, number of MNs, the length and width aspect ratio and surface area (Al-Qallaf & Das, 2008, 2009; Olatunji et al., 2012, 2013; Guo et al., 2013). It has been suggested that MNs can be adapted to aid lidocaine delivery yielding many fold increase in delivery rate (Kwon, 2004; Li et al., 2008; Wilson et al., 2008; Zhang et al., 2012a, b; Kochhar et al., 2013; Ito et al., 2013; Nayak et al., 2014).

A number of studies have successfully delivered numerous active molecules using MNs, e.g. hepatitis B vaccine (Guo et al., 2013), Solaraze[®] gel in extending pore opening (Ghosh et al., 2013b) and naltrexone co-drug with diclofenac drug (Banks et al., 2013). In another recent study, it has been shown that MNs can be combined with ultrasound for increasing the delivery rate of a large macromolecular drug (Han & Das, 2013). These studies have directed the hypothesis that MNs and ultrasound combination could be used for greater epidermal lidocaine delivery in order to determine the significance of optimum sonophoretic power-related effects on lidocaine permeation.

In this context, it is important to state that sonophoresis is generally based on ultrasound frequency. The low frequency sonophoresis (LFS) is defined to be within 20–100 kHz and the high-frequency sonophoresis is usually for above 0.7 MHz (Polat et al., 2011). The mechanism by which enhanced permeability is achieved via ultrasound can be linked to a number of physical phenomena, including thermal effects, formation of cavitation, mechanical effects and convective localized fluid velocities in skin. However, in the ultrasound pre-treatment experiment, it is generally accepted that inertial cavitation is the largest contributor to the enhancement in skin permeability. It is more so with LFS as described by Merino et al (2003) due to larger bubble size at low frequency range. Inertial cavitation occurs due to pressure variations induced by ultrasound, resulting in rapid growth and collapse of bubbles formed in the coupling medium. The collapsing of the aforementioned bubbles near skin surface will cause micro-jets due to asymmetrically release of energy. These micro-jets have been confirmed as the main contributors to the permeability increment (Wolloch & Kost, 2010). The effects of ultrasound have been studied for the enhancement of transdermal lidocaine delivery with significant results for both pulsed and continuous output mode of LFS (Ebrahimi et al., 2012). However, as far as we are aware of, these techniques are yet to be combined and studied for permeability enhancement levels, particularly for lidocaine.

The potential for MN-assisted lidocaine delivery via hydrogel microparticles was discussed with the conclusion that there is significant commercial potential for lidocaine MNs (Zhang et al., 2012a, b; Nayak et al., 2014). Polymeric hydrogel microparticles are good for the purpose of controlling spreading (i.e. controllable spreading radius, droplet

height and contact angle) of the drug formulation over skin (Nayak et al., 2014).

In this particular study, the drug vehicle for lidocaine encapsulation is polyanionic, carbohydrate-based NaCMC cross-linked with polycationic, protein-based gel in forming a hydrogel (Nayak et al., 2014). Previously lidocaine formulation bypassing the SC epidermal layer was outlined, the viscoelastic properties in adapting a NaCMC/gel network hydrogel prevent slippage of the drug formulation when applied to the skin and the possibility of non-convective flow through the opened cavities of the skin from MN treatment (Milewski & Stinchcomb, 2011; Ghosh et al., 2013a). To try and exploit this potential, the main aim of the study is to combine the techniques in MN array and ultrasound technology as a pre-treatment to meet the definition of an ideal anaesthetic delivery method. A major advantage is that an extended release is possible using this approach. A carbohydrate-based visceral hydrogel formulation was prepared as a model anaesthetic as this provides flexible properties and ability to encapsulate considerable amounts of liquid drug, lidocaine in this instance (Milewski & Stinchcomb, 2011), as discussed in the following section. Furthermore, the spreading behavior of the prepared formulation was studied and compared with the spreading behavior lidocaine solution as a Newtonian liquid. Unlike numerous studies performed using synthetic substrates, this study implements porcine skin as a lipophilic substrate as was attempted by Chow et al. (2008).

Materials and methods

NaCMC and gel emulsion was cross-linked to form hydrogels with encapsulated lidocaine in batch scale production. This formulation setup is highly beneficial because of fairly efficient preparation times in achieving a finished drug formulation and low heat treatment in adaptation of green chemistry.

Materials and equipments

Sodium carboxymethylcellulose (D.S. 0.9; M.W. 250 kD), sorbitan mono-oleate (SPAN 80), glutaraldehyde 50% w/w, paraffin liquid (density range: 0.827–0.89 g/ml), lidocaine (M.W. 288.81 g/mol), methylene blue (50% v/v) and porcine gelatine (type A) were purchased from Sigma Aldrich Ltd (Dorset, UK). Analytical grade acetic acid, high-performance liquid chromatography (HPLC) grade acetonitrile and n-hexane (95% w/w) were purchased from Fisher Scientific UK (Loughborough, UK). A Gemini-NX column (C18) of particle size 3 µm was purchased from Phenomenex (Cheshire, UK) for HPLC instrumentation. Amputated porcine ears (age of pig: 5–6 months) were purchased from a local butcher and dissected into 20 mm × 20 mm squares before storage at -20 ± 1 °C. Also, 10 mm × 10 mm squares of same porcine skin were dissected as a substrate for droplet spreading. MN patch (stainless steel, flat arrow head geometry and 1100 µm length) was purchased from nanoBioSciences (Sunnyvale, CA). Branson Digital Sonifier 450 (Danbury, CT) was chosen as the ultrasound output system. This ultrasound system includes an auto-calibrated transducer and a digital output controller. The frequency of the ultrasound is fixed at 20 kHz but the output powers are

adjustable between 4 and 400 W. The equipment for droplet spreading studies was AVT Pike F-032 high-performance camera (Allied Vision Technologies UK), Camera i-speed LT high speed video (Olympus, UK).

Formulation of lidocaine NaCMC/gel hydrogel

Paraffin oil (100 ml) was sheared continuously for up to 400 rpm in a stirred vessel bought from IKA (Staufen, Germany). Span 80 (0.5% w/w) was dispensed in ambient conditions. To this, NaCMC (1.24% w/w) in ultrapure water was added drop-wise, and depending on the polymeric ratio (c % w/w), gel in ultrapure water was also added drop-wise at 35–40 °C (Table 1). A subsequent pH reduction of the solution to pH 4.0 was performed by the addition of acetic acid (~3% w/w). While shearing at 400 rpm, lidocaine HCl (2.44% w/w) was added drop-wise in ultrapure water at 20 °C into the polymer mixture. The polymeric mixture was then cooled to 5–10 °C for 30 min to initially harden the microparticles. Glutaraldehyde (0.11% w/w) was added to the emulsion as a cross linker. Upon returning to 20 °C temperature, the hydrogel mixture was sheared for 2 h at approximately 1000 rpm to ensure thorough mixing. The lidocaine NaCMC/gel formulation was then left to stand until a distinct w/o boundary was observed after which this formulation was left overnight at 1–5 °C. Excess paraffin liquid was removed via n-hexane separation shaking (50% v/v); top organic layer was discarded before placing the hydrogel formulation in a vacuum oven (Technico, Fistreem International Ltd, Loughborough, UK) under full vacuum and a temperature of 20 °C for 8 h. Following this, the formulation was washed with deionized (DI) water and filtered using commercial filter papers with pore size 6 µm (Whatman, Ltd, Oxon, UK) for the removal of unbound lidocaine before further characterization. In the case of F5 residual paraffin and n-hexane were removed by rotary evaporation (Heidolph Instruments, Essex, UK). Similarly, the formulation was washed with DI water and filtered as previously outlined.

Zeta potential of lidocaine NaCMC/gel hydrogel

The zeta potential was measured using a Zetasizer (3000 HSa, Malvern Instruments, Worcestershire, UK). Lidocaine NaCMC/gel (2.0 ± 0.5 g/ml) in DI water was injected into the sample port, temperature maintained at 25.0 °C and the results were obtained in triplicate. The zeta-potential (ζ) was measured in terms of electrophoretic mobility (μ) via an optical technique, and ζ (mV) (Park et al., 2005) of the diluted hydrogel was computed from the Smoluchowski equation, where μ is the referenced with latex ($\text{m}^2 \text{v}^{-1} \text{s}^{-1}$), η is the DI volume viscosity ($\text{m}^2 \text{s}^{-1}$), ϵ_0 and ϵ_r are the

permittivity in a vacuum and relative permittivity of DI water as medium, respectively (Sze et al., 2003)

$$\zeta = \frac{4\pi\mu\eta}{(\epsilon_r\epsilon_0)} \quad (1)$$

Viscometric analysis of lidocaine NaCMC/gel hydrogel

A well-mixed sample volume (25 ml) of lidocaine NaCMC/gel hydrogel sample was determined for variations to viscoelastic properties at standard temperatures of 20 °C. An inducing shear rotating viscometer (Viscotester VT550, Haake, Germany) with rotor and cup (NV1) assemblies and a constant ravine of 0.35 mm, in between the assembly was adapted in viscometric analysis. More details on this aspect of our work are presented by Nayak et al. (2014).

Optical micrographs of lidocaine NaCMC/gel hydrogel

Micrographs were obtained using an optical microscope (BX 43, Olympus, Southend-on-sea, UK) and a camera attachment captured colored still images (Retiga-2000R, QImaging, British Columbia, Canada). Micrographs were pictured in triplicate for each formulation. An image processing software (*ImageJ*) was adapted in pixel measurement via graticule calibration to interpret particle size diameters from a random selection of 50 microparticles per image. ImageJ is a Java-based open source image processing and analysis program developed at the National Institute of Health (NIH), USA.

Controlled release of lidocaine from NaCMC/gel hydrogel

Lidocaine NaCMC/gel hydrogel (0.1 ± 0.05 g) was placed in an amber vial and 25.0 ml of DI water was dispensed before the sample was placed in a pre-heated thermo-stat bath at 37.0 ± 0.5 °C (Grant Instruments, Cambridge, UK). Subsequently, 1 ± 0.0005 ml of heated sample removed by autopipette (Eppendorf, Stevenage, UK), filtered using Nylon membranes (Posidyne, 0.1 µm) and analyzed for lidocaine content using HPLC instrumentation. The results were measured in triplicate and the standard deviation from sample mean was taken.

Ex vivo skin permeation study of lidocaine NaCMC/gel hydrogel

Jacketed Franz diffusion cells (FDC) (Logan Instruments, NJ) were used as previously annotated for determining the *ex vivo* drug permeation rate through porcine skin (Nayak et al., 2014). Porcine ear skin was used in this analysis because of the histological similarity with human skin. Dissected square

Table 1. Lidocaine NaCMC/gel hydrogel mass ratio with particle size values.

Sample ID	NaCMC (% w/v)	Gelatine (c % w/w)	Lidocaine (% w/w)	NaCMC/gelatine ratio	Drier type	Mean particle diameter ± S.D. (µm)	Particle diameter range (µm)
F1	1.2	2.0	2.4	1:1.6	Vacuum	5.89 ± 0.0026	1–13
F2	1.2	2.4	2.4	1:2.00	Vacuum	6.04 ± 0.0027	1–14
F3	1.2	2.8	2.4	1:2.33	Vacuum	6.81 ± 0.0029	2–17
F4	1.2	3.2	2.4	1:2.67	Vacuum	7.42 ± 0.0029	3–17
F5	1.2	3.2	2.4	1:2.67	Rotary	14.60 ± 0.0067	4–31

skin sections (20×20 mm) were defrosted at 25°C for a maximum time of 1 h before the commencement of this study. The FDC receptor chamber (5.0 ml) was filled with DI water and constantly stirred using a magnetic flea. The FDC receptor volume was constantly maintained at $37 \pm 1^\circ\text{C}$ through a water jacket. A square section of full thickness skin (subcutaneous fat and connective tissue removed) was placed on the top of the aperture surface of diffusion cell with a diffusion area of 1.33 cm^2 . The average skin thickness was recorded in the range of $760\text{--}787\ \mu\text{m}$ ($\pm 25\ \mu\text{m}$). The continuous viscoelastic properties of skin are unlikely to allow for MNs to penetrate beyond $200\ \mu\text{m}$ when considering $1500\ \mu\text{m}$ needle length rollers penetrating a depth of $150\ \mu\text{m}$ (Roxhed et al., 2007; Badran et al., 2009). The lidocaine NaCMC/gel hydrogel ($0.10 \pm 0.03\text{ g}$) was placed on to the skin's donor compartment, the split second timer initiated and then the skin was securely clamped with a donor lid. A fixed 1.5 ml receptor volume was syringe removed periodically from the receptor chamber and replaced with 1.5 ml of DI water. Following this, the samples were analyzed for free lidocaine using HPLC instrument (Agilent 1100 series, Hewlett Packard, Santa Clara, CA). A similar FDC method was used for all drug release experiments concerning passive diffusion, MNs only pre-treatment, LFS only pre-treatment, MNs and LFS pre-treatment. MNs were carefully applied to the skin ensuring penetration and held in place using a constant pressure device comprising a pneumatic piston (0.05 MPa) for 3 or 5 min. LFS was supplied for pre-treatment only using a probe set to 20 kHz frequency for 5–10 min. Continuous mode of ultrasound was chosen due to no significant difference being observed during pre-treatment applications (Herwadkar et al., 2012). The inter-coupling distance between the skin and probe was set to 2 mm with coupling medium of DI water. In the case of MNs combined with ultrasound pre-treatment, the MN patch is applied before the ultrasound treatment. A minimum lidocaine concentration of $1.5\ \mu\text{g}/\text{ml}$ was deduced from the literature as the permissible effective drug therapeutic value in plasma (Grossman et al., 1969; Schulz et al., 2012).

Spreading of lidocaine NaCMC/gel 1:2.33 across porcine skin

The setup for measurement of spreading radius, droplet height and apparent contact angle of droplet was similar to Chao et al. (2014). A square section of porcine skin ($10\text{ mm} \times 10\text{ mm}$) was placed flat in a closed sample box. A sample

droplet ($3.0 \pm 0.5\ \mu\text{l}$) was dispensed on the porcine skin, camera frame rate capture of 1.85 frames per second (fps) was maintained and the results recorded. Results were obtained in duplicate for the optimum particle size-controlled formulation and compared with a duplicate set of lidocaine solution of the same lidocaine loading weight (2.44% wt).

Histological study

The determination of MN insertion depth into skin by post MN treatment of skin was adapted from Cheung et al. (2014). First, the skin sample is pre-treated using $1100\ \mu\text{m}$ MN patch for 5 min. Then, the porcine skin sample is stained using methylene blue (50% v/v) and merged into embedding compound (Bright Cryo-m-Bed, Huntingdon, UK) which is filled in a cuboid mould. The whole sample is then put inside the microtome (Bright Cryostat 5030, Huntingdon, UK) to solidify. The frozen sample is cut into $15\ \mu\text{m}$ slices and analyzed under the microscope for the histology.

Results and discussions

Lidocaine NaCMC/gel hydrogel microparticle size diameters and morphology

Lidocaine encapsulated hydrogel microspheres based on NaCMC and gelatine were prepared using glutaraldehyde in transforming emulsion droplets to defined microparticles. As the mechanisms for ionic interactions in forming spherical microparticles are known (Gupta & Ravi Kumar, 2000; Berger et al., 2004), it is not discussed in detail in this paper. The morphological observations of lidocaine NaCMC/GEL microparticles are spherical, well-formed and slightly agglomerated for a significant number of them (Figure 1A and 1B). Mean particle size diameters (Table 1) in the formulation ranged from 5.89 to $14.60\ \mu\text{m}$ depending on the formulation with an increase in mean particle size observed with an increased gelatine ratio. This is the likelihood of increased gelatine component of the hydrogel, producing larger droplets during the w/o emulsification and subsequent hardening after the addition of glutaraldehyde. The rotary evaporation method yielded significantly larger particle sizes in comparison to vacuum drying. Interestingly, a positively skewed particle size distribution was observed for all lidocaine hydrogel formulations (Figure 2).

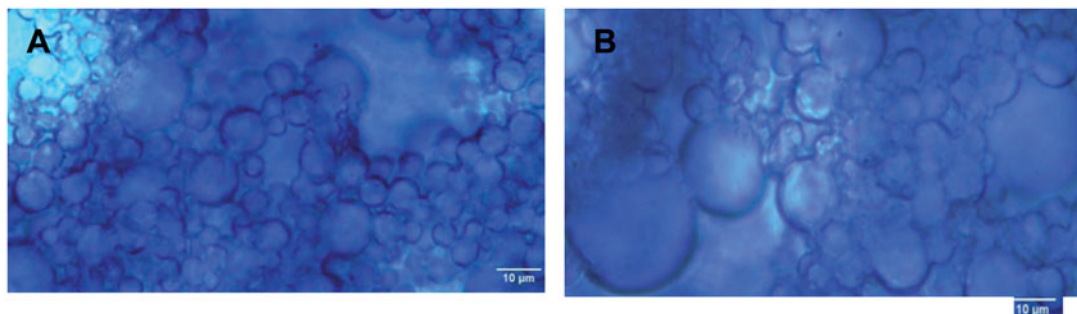


Figure 1. Micrograph of (A) lidocaine NaCMC:gel 1:2.33 hydrogel showing distinctly formed microparticles. (B) Lidocaine NaCMC:gel 1:2.66 hydrogel showing larger and slightly more agglomerated microparticles.

Dispersion of lidocaine NaCMC/gel hydrogel microparticles

Zeta potential studies in lidocaine NaCMC/gel hydrogels demonstrated a stable and fairly dispersed microparticulate system. The results (Figure 3) expressed a trend of decreasing stability with an increase in the gelatine ratio, which in theory should impact a greater level of microparticle agglomeration thus likely affecting the permeability through skin. The pH of all formulations was kept constant and therefore it should not have affected the zeta potential although the slight decline of ζ -potential in the positive direction is linked to the increase

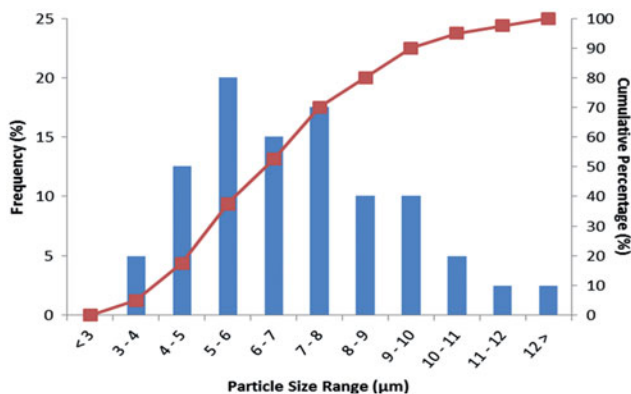


Figure 2. Particle size distribution of Lidocaine NaCMC/gel hydrogels.

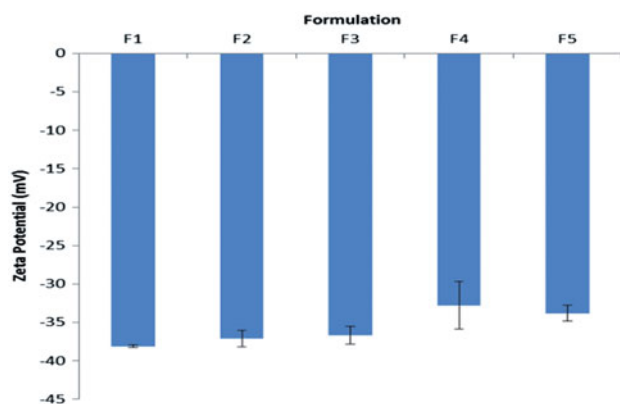
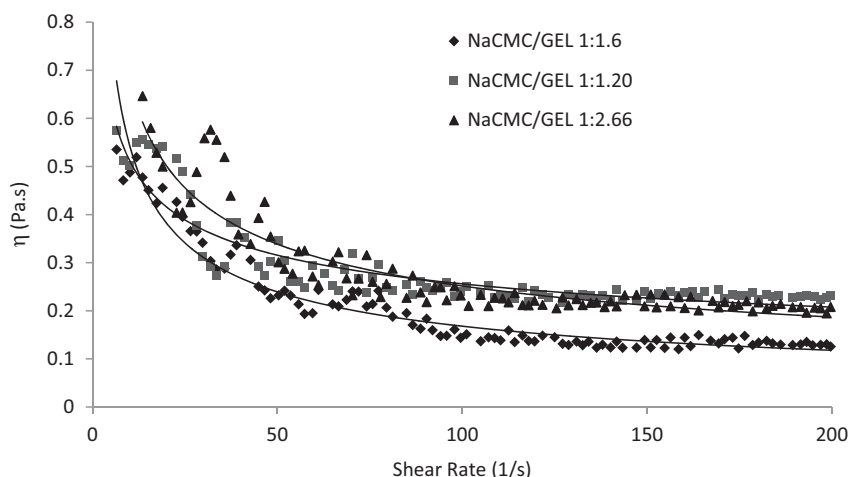


Figure 3. Lidocaine NaCMC/GEL 1:1.6–1:2.66 (F1–F4) and lidocaine NaCMC/GEL 1:2.66 by rotary evaporation prep. (F5) for zeta potential.

Figure 4. Lidocaine 2.44% w/w NaCMC/GEL ratio pseudo-plasticity.



in gelatine ratio caused by gelatine in conjunction to lidocaine possessing a positively charged tertiary amide group at pH 4.0 and thus contributing to the increasing negative surface charge. The anionic polymer, sodium carboxymethyl cellulose has a ζ -potential value of -30 mV (Ducel et al., 2004) and electric charge neutralization did not occur or was not significantly induced by gelatine or lidocaine, so the overall lidocaine NaCMC/gel hydrogel charge was greater than -30 mV. Nevertheless, reduced agglomeration is the result of a medium pKa, higher dielectric constants in comparison to a polymeric hydrogel components converging to significantly low overall ζ -potential range of -35 to -40 mV and the effect of electrostatic particle repulsion (Xu et al., 2007).

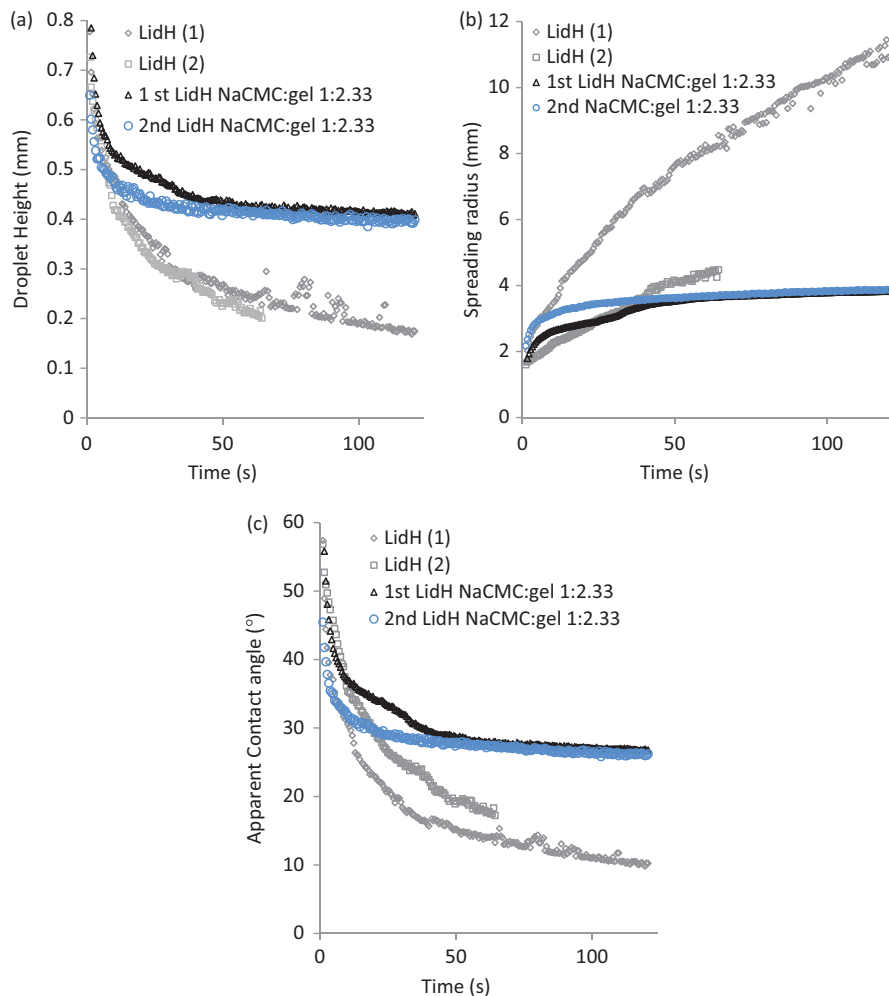
Viscoelasticity of lidocaine NaCMC/gel hydrogel

Viscosity determination (Figure 4) revealed a lenient pseudo-plastic nature for the formulation with lidocaine NaCMC/gel hydrogel with good correlative best fit curves observed for individual set of data points ($R^2 > 0.93$). The dynamic viscosity plots showed similar mild pseudo-plastic behavior between the formulations with lidocaine NaCMC/gel 1:2.66 hydrogel being marginally higher when considering the upper viscosity range of 0.5 – 0.6 Pa s at a starting shear of 25 s $^{-1}$ and then more defined shear thinning behavior observed above 100 s $^{-1}$. Lidocaine with sodium carboxymethylcellulose as a polyanionic vehicle alone will not be sufficient in enhancing pseudo-plastic properties and a recent study has shown that the profile of a dynamic viscosity plot is Newtonian (Alaie et al., 2013).

Control of lidocaine NaCMC/gel 1:2.33 spreading on porcine skin

The spreading radius and height of lidocaine NaCMC/gel 1:2.33 outline significant control on its spreading behavior compared with lidocaine solution of the same mass loading (Figure 5a and 5b). The beginning of the plateau effect is observed after 10 s and therefore, there is expected to be a localization effect on the skin surface (Figure 5a and 5b). The apparent contact angles of lidocaine NaCMC/gel 1:2.33 droplets are considerably higher than the lidocaine solution contact angle droplets, near to the skin impact time of 0 s (Figure 5b). Apparent contact angle stability is noticed after

Figure 5. Lidocaine NaCMC/gel 1:2.33 comparison with Newtonian lidocaine solution according to (a) droplet heights (b) spreading radii (c) apparent contact angles. The results suggest that the spreading of lidocaine NaCMC/gel 1:2.33 on the skin surface is much more predictable/controllable as compared with lidocaine solution.



40 s (Figure 5c). Our results also show that the lidocaine solution is a Newtonian liquid that can spread much faster than lidocaine NaCMC/gel microparticles.

The percentage release of lidocaine from controlled release of lidocaine

All four lidocaine NaCMC/gel hydrogels outline rapid release of lidocaine directly in DI water during the first 1 h with steady state conditions observed in the next 3 h (Figure 6a). A 0.3 fold decrease in cumulative release is observed in the first hour when comparing lidocaine NaCMC/gel 1:1.6 with lidocaine NaCMC/gel 1:2.66 as the highest releasing outline. Also, a 0.1 fold decrease in cumulative release was observed in the next three hours when comparing lidocaine NaCMC/gel 1:1.6 with lidocaine NaCMC/gel 1:2.66. This shows that the variation between hydrogel ratios is not significantly large as permeation release profiles explained in the following sections. The percentage release of lidocaine from NaCMC/gel hydrogels was determined by the following:

$$\text{Percentage drug release} = \frac{M_s - M_t}{M_s} \times 100, \quad (2)$$

where M_s is the maximum mean cumulative steady state concentration of drug and M_t is the mean cumulative concentration of lidocaine taken specifically at release time. The highest amount of Lidocaine released was from

NaCMC/gel 1:1.6 hydrogel in which 32.3% was detected in the DI water media in one hour (Figure 6b). This is because the smaller particles sizes of Lidocaine NaCMC/gel 1:1.6 ratio allow for a greater surface area and encapsulated lidocaine thus rapidly dissolves in DI water. The lidocaine NaCMC/gel 1:2.66 ratio comprises larger microparticles and therefore a smaller surface area is exposed for DI water dissolution so the percentage of lidocaine released was 17.4% in one hour. Significantly less amounts of lidocaine is released for all NaCMC/gel hydrogel formulations after 1 hour reflecting the steady state conditions of the hydrogel as the DI water media becomes a saturated solution.

Histological analysis on the MNs

The MNs that are employed in the histological experiment are 1100 μm in length. The purpose of the histological experiment is to determine the insertion depth of this MN patch under thumb pressure for which post-MN-treated skin is micrograph imaged (Figure 7). According to Figure 7, the insertion depth is between 300 and 400 μm which are much lower than the real length of MNs. This is caused by several reasons, such as the viscoelastic properties of the skin, the geometry of the MNs and the insertion force. This reduced insertion depth can further affect the permeation results.

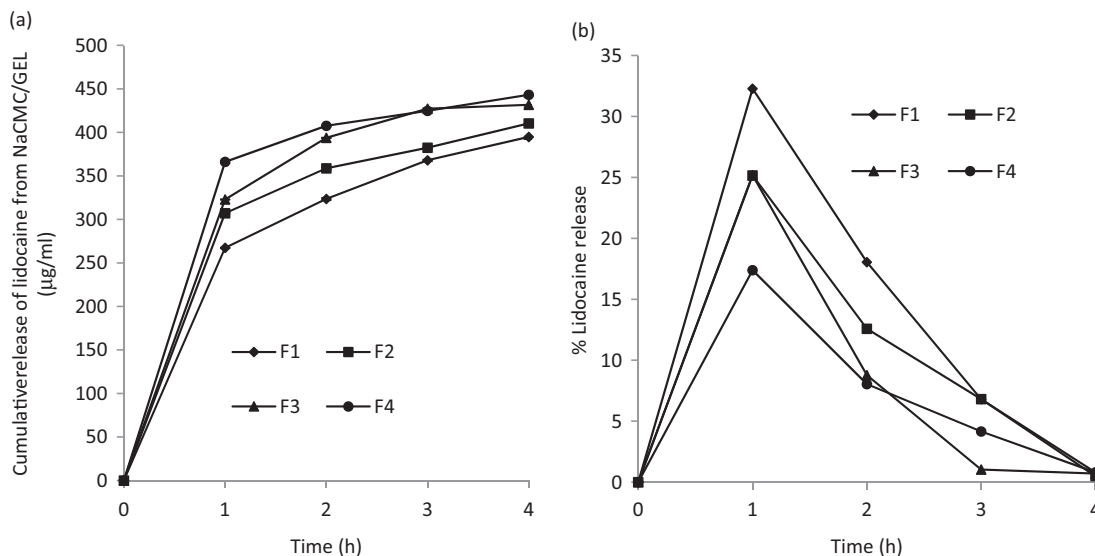


Figure 6. The controlled release of Lidocaine 2.44% w/w encapsulated (a) NaCMC/GEL 1:1.6 (F1), NaCMC/GEL 1:2.0 (F2), NaCMC/GEL 1:2.33 (F3) and NaCMC/GEL 1:2.66 (F4) (b) as a percentage into DI water medium from NaCMC/GEL 1:1.6 (F1), NaCMC/GEL 1:2.0 (F2), NaCMC/GEL 1:2.33 (F3) and NaCMC/GEL 1:2.66 (F4). The error bars in (a) the standard deviation of mean represents the error. (b) No error bars indicated.

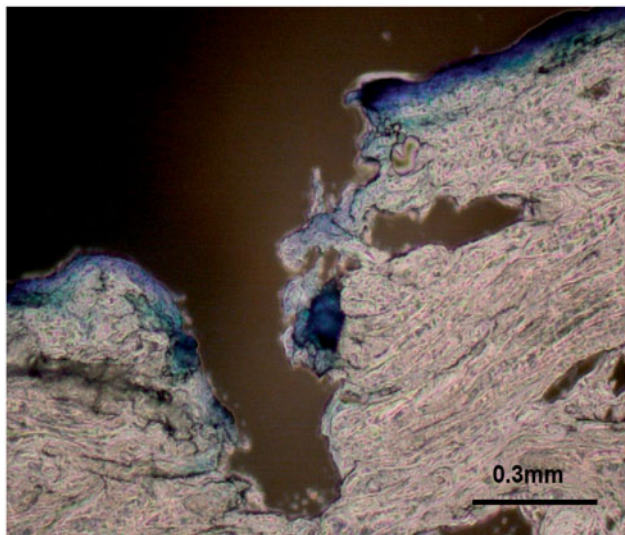


Figure 7. The MN insertion depth of skin sample using 1100 µm MNs under thumb pressure. The histological studies show that although the MNs are 1100 µm, for the MN density in the array and force applied, they create holes of approximately 400 µm.

Passive diffusion of lidocaine NaCMC/gel hydrogel

Skin passive diffusion experiments were carried out in order to provide a control from which any pre-treatment enhancement results can be compared and contrasted. The lowest polymeric microparticle ratio 1:1.6 of lidocaine (Figure 8a) outlines the most desirable cumulative permeation for lidocaine in crossing the minimum threshold therapeutic level after 0.57 h. This is the shortest lag time for reaching the pain receptors for lidocaine in the deep dermis region rich in watery plasma and nerves. The hydrogel microparticle chemistry is a combination of significantly high negative zeta potential and smaller mean particle size contributing to an increased permeation. All lidocaine NaCMC/gel ratio

hydrogels have demonstrated a very low initial permeation at a maximum of 0.3 µg/ml reached in 0.5 h. This is the normal lag time because of a longer path length for microparticle permeation when considering the topmost SC layer surface area bigger than the accessible viable epidermis (VE) layer microcavities. However, lidocaine NaCMC/gel 1:2.0 and lidocaine NaCMC/gel 1:2.66 hydrogels are the next two favorables after the most desirable formulation containing a polymeric mass ratio 1:1.6 for bypassing the minimum therapeutic threshold at a shorter time interval. Initially, lidocaine is diffusing through the fresh skin because of microparticulate disruption to the hydrogel formula caused by natural skin moisture hence the low initial concentration rates proceeding upto 0.5 h. Due to the requirements of lidocaine as an fast acting anaesthetic, the current results confirm enhancement of permeation is required if minimum therapeutic threshold of lidocaine (1.5 µg/ml) are to be reached within a suitable time frame for this technique to be of practical use. The lag time to cross a minimum therapeutic level is slightly greater than 1 h in lidocaine NaCMC/gel 1:2.33 hydrogel and just over 2 h for lidocaine NaCMC/gel 1:2.66 hydrogel, a rotary evaporation method with respect to passive diffusion alone which is considerably a long, unreasonable waiting time for a promising polymeric hydrogel ointment drug. The cumulative lidocaine thresholds tend to stabilize post 4 h, where equilibrium is reached and no more drug is released into the concentrated dermal region. This means that the lidocaine hydrogel ointment can be washed off the skin.

FDCs are *in vitro* glass cells in which soluble drugs can dissolve in a known volume of liquid solvent before timed removal and replacement of fresh solvent. The challenges in using FDCs are minimizing the occurrence of trapped air during the replaced of a volume of dissolved drug solution with fresh solvent (Sintov & Shapiro, 2004). Also large trapped air bubbles may be observed sometime while placing sectioned skin sample across the aperture of the receptor

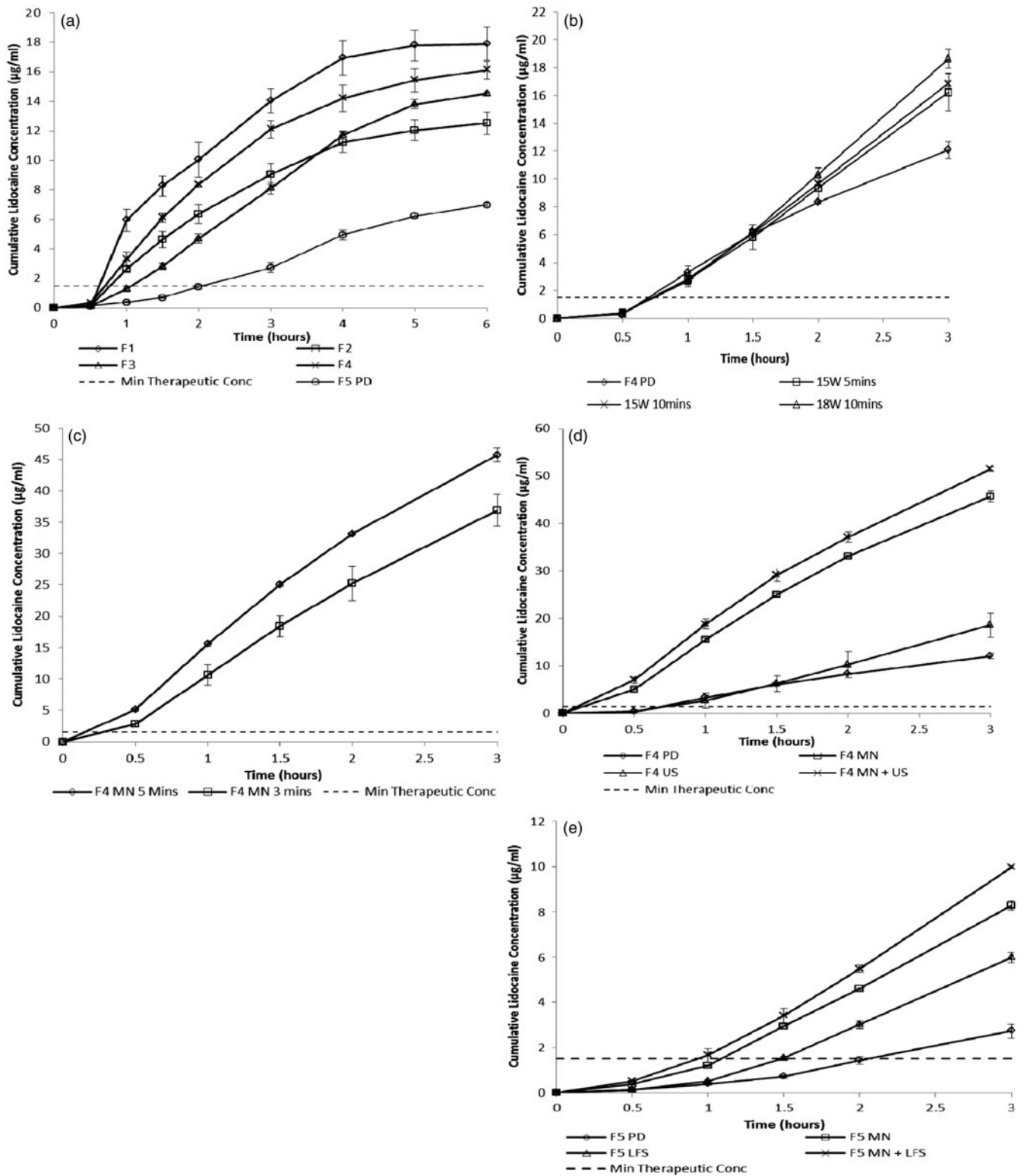


Figure 8. Cumulative lidocaine permeation from Lidocaine. (a) NaCMC/GEL 1:1.6 (F1), NaCMC/GEL 1:2.0 (F2), NaCMC/GEL 1:2.33 (F3), NaCMC/GEL 1:2.66 (F4) and passive diffusion (PD) NaCMC/GEL 1:2.66 by rotor evaporation prep stage (F5). (b) F4 PD and comparative pre-treatment with ultrasound at 15 W and 18 W for 5 and 10 min, respectively. (c) F4 adapting a MN patch for a 3 min and 5 min pre-treatment duration for Lidocaine NaCMC/GEL 1:2.66. (d) F4 adapting NaCMC/GEL 1:2.66 (F4 PD), NaCMC/GEL 1:2.66 (F4 US, 18 W 10 min), NaCMC/GEL 1:2.66 (F4 MN, 5 min) and NaCMC/GEL 1:2.66 (F4 MN 5 min and US 18 W 10 min). (e) NaCMC/GEL 1:2.66 (F5 PD), NaCMC/GEL 1:2.66 (F5 LFS, 18 W 10 min), NaCMC/GEL 1:2.66 (F5 MN, 5 min) and NaCMC/GEL 1:2.66 (F5 MN 5 min, LFS, 18 W 10 min).

chamber. Overfilling the receptor aperture by 0.4 ml minimizes the introduction of large air bubbles.

Lidocaine NaCMC/gel hydrogel was compared with lidocaine solution permeation from the literature (Sekkat

et al., 2004). Prior to this passive diffusion comparison with lidocaine solution passive diffusion, the permeation units of $\mu\text{g/ml}$ were converted into $\mu\text{g/cm}^2$ by the product of the known receptor volume followed by the quotient of the

adjustment factor value of 2.36 ($3.14 \text{ cm}^2/1.33 \text{ cm}^2$) due to the increase in FDC diffusion area when comparing a similar study using a smaller aperture diameter (Sekkat et al., 2004). The current lidocaine NaCMC/gel 1:1.6 hydrogel crosses the minimum therapeutic threshold by 1.8 fold than lidocaine solution on similar full thickness skin despite lidocaine solution permeating initially at 1.4 fold faster before a half an hour time frame and not anywhere near the minimum therapeutic threshold (Sekkat et al., 2004). Most FDC techniques appear a commonplace for PD studies and there is still a relatively big gap in adopting FDCs for MN-based permeation studies. Lidocaine NaCMC/gel 1:2.66 and lidocaine NaCMC/gel 1:2.66 hydrogel formulated by rotary evaporation were chosen to be studied for further enhancement via pre-treatment. The factor of permeation enhancement can be deduced when making this comparison.

Ultrasound only pre-treatment of lidocaine NaCMC/gel ratio 1:2.66 hydrogel

To observe the effect of power and application time of LFS has on permeation, LFS was applied continuously with varying power and exposure time as shown in Figure 8(b). Theoretically, the exposure of LFS should form inertial cavities in the coupling medium and develop micro-jets toward the skin surface to aid permeation. However, lidocaine transport through the skin saw no significant enhancement up to 2 h after which a significant enhancement, especially power induction, 18 W at 10 min for lidocaine NaCMC/gel 1:2.66 (T -test $p < 0.026$) outlined a greater permeation profile. The results conclude that an increase in power has a greater enhancement effect compared with an increase in LFS exposure time; however, no significant increase in lidocaine transport through the skin was observed during the initial stages after varying respective power induction and time durations while maintaining constant NaCMC/gel ratios of lidocaine hydrogel drug application. It is predicted that a higher LFS power level would further increase diffusion; however, the risk of thermal effects would be too high for this to be of practical use.

MN pre-treatment of lidocaine NaCMC/gel ratio 1:2.66 hydrogel

PD permeation (Figure 8d) and MN-assisted permeation (Figure 8c) with a post application time limit of 3 and 5 min concurrently were compared altogether. MN only pre-treatment of lidocaine NaCMC/gel 1:2.66 hydrogel generated a substantial increase in lidocaine permeation for both the 3 and 5 min post MN duration (Figure 8c). A statistically significant difference ($p < 0.04$) was observed for MN application duration. Initial ($t = 0.5 \text{ h}$) permeation for the 3 and 5 min patch duration resulted in increases of 9 and 17 fold, respectively. An average 3 fold increase in permeation was observed for the 3 min MN application and comparatively an increase by 4 fold for a 5 min MN application. The results indicate that therapeutic levels of lidocaine could be reached within 0.15 h or 9 min post application MN, in comparison to no pre-treatment requiring 40 min (Figure 8c and 8d). The reason for this short lag time is due to

lidocaine microparticles traveling at a shorter path length to the deep dermis layer. The SC layer has been bypassed by artificial MN cavities. MN-assisted cumulative release study with respect to lidocaine formulations has not been performed *ex vivo* to date. However, *in vivo* release studies have been performed using non degrading polymeric MN array coating of lidocaine alone, sustained approximately 15 min of delivery thus proven successful for rapid emergency anaesthesia (Zhang et al., 2012a, b). *In vivo* release studies with *ex vivo* cumulative release studies are completely incomparable due to obvious differences in experimental procedures and removal of active drug for characterization. The lidocaine NaCMC/gel 1:1.6 ratio (Figure 8a) hydrogel crosses the therapeutic level at significantly slower time duration, greater than 30 min in lidocaine NaCMC/gel 1:2.66 ratio in comparison of MN and LFS treatment. This is due to the fact that MNs and ultrasound are involved in either cavity engulfing of larger sized hydrogel microparticles.

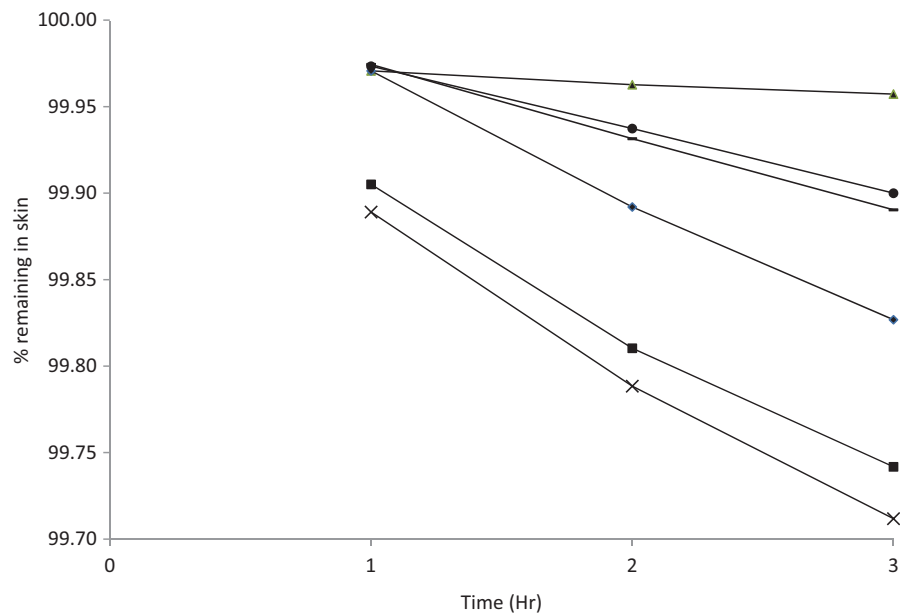
MN and ultrasound (dual) pre-treatment of lidocaine NaCMC/gel ratio 1:2.66 hydrogel

Both pre-treatments (dual) were combined and studied for further permeation enhancement in comparison to MN or LFS pre-treatment only. Lidocaine NaCMC/gel 1:2.66 hydrogel in which combining a 10 min application of 18 W LFS after a 5 min application of MNs demonstrated an initial faster permeation by 23 fold with an average 4.8 fold increase over 30 min of application when compared with separate device treatments and passive diffusion (Figure 8d). Therapeutic levels of lidocaine could theoretically be reached after 7 min post application in terms of reaching the deep dermis layer of skin as the target. A general increase in permeation throughout the period of experimentation can be noticed rather than post 2 h as seen with LFS pre-treatment only, this could be due to efficiency of LFS pre-treatment is further enhanced on porous skin sample formed via the MN patch.

Dual pre-treatment of lidocaine NaCMC/gel 1:2.66 hydrogel via a rotary evaporation method

Lidocaine NaCMC/gel 1:2.66 hydrogel with the rotary evaporation method as described earlier, favored an additional time of nearly 0.9 h or 50 min after the application of 18 W LFS at 10 min ($p < 0.04$) to reach minimum therapeutic level in conjunction to a two fold average increase in permeation after 1 h, compared with the same formulation without rotary evaporation method (Figure 8d and 8e). This was the likelihood of higher heating temperatures compromising the glutaraldehyde fixation and thus resulting in larger microparticle as previously reported. Higher heating temperatures were required in the large volume removal of n-hexane and paraffin oil mixture by solvent evaporation. A 5 min application of the MN array led to an initial increase by 2.8 fold and subsequently an average 3.4 fold increase was observed with respect to the deep dermis layer skin target. Combining the two pre-treatments resulted in an initial permeation increase by 3.8 fold followed by an average increase by 4.1 fold in comparison to passive diffusion only (Figure 8d and 8e). Therapeutic levels of

Figure 9. Percentage of lidocaine contained in (F4) NaCMC/GEL 1:2.66 (passive diffusion), (MNs, 3 min), (MNs, 5 min), (LFS 5 min 15W), (LFS 10 min 18 W), (MN + LFS). (Error bars outline a random error range of 0.005%).



lidocaine were reduced from just over 2 h to less than 1 h on average.

Mass transfer of lidocaine from NaCMC/gel 1:2.66 hydrogel

The percentage of lidocaine remaining inside *ex vivo* skin was determined by the subtraction of the mass of lidocaine initially encapsulated during formulated preparation (125 000 μg) by the cumulative amount detected in DI water from controlled release studies. The purpose of using controlled release studies is to determine the amount of lidocaine contained in the vehicle as mass balance before the subtraction of the mass of lidocaine in the receptor in which the DI water in the receptor is the deep dermis. All mass balances were carried out in μg and converted from cumulative concentration units of $\mu\text{g}/\text{ml}$ before the percentage of lidocaine remaining inside the skin was determined (Figure 9). Overall the mass transfer of lidocaine with respect to all treatment applications appeared to outline a gradual, a slow process of diffusing through the full thickness appendage. However, there is a fairly substantial decline in the percentage of lidocaine remaining in the skin when MN and ultrasound treatment (LFS) method was applied. This can be interpreted as diffusion of lidocaine molecules through skin cells and layers before clearance into the blood stream. The lowest percentage of lidocaine remaining in the skin is 99.7% after a time of 3 h (Figure 9).

Conclusions

This study aimed to use LFS and MNs as a pre-treatment to skin in order to enhance permeation of lidocaine encapsulated in a formulation. A significantly more microparticle stability was found with lower gelatine ratios (1:1.60); however, all formulations were sufficiently stable (zeta potential: $\geq -30\text{ mV}$). Our diffusion experiments revealed a small increase in diffusional permeation when LFS was used in combination with a MN array pre-treated skin. However,

rotary evaporation during the final polymeric drug formulation stage caused significant reductions in lidocaine permeation levels. Nota bene that the main purpose for utilizing rotary evaporation was for reduced time in the removal of a large volume of residual paraffin and n-hexane as the final operative method compared with vacuum oven drying (data not shown). Lidocaine NaCMC/gel 1:2.66 and lidocaine NaCMC/gel hydrogel 1:2.66 formulated by rotary evaporation showed a decreased time required to reach minimum therapeutic levels of lidocaine by 5.7 and 2 fold, respectively. Generally, lidocaine permeation was significantly increased with higher sonophoresis power and increasing exposure duration demonstrated a minor increase in the permeation rate for lidocaine NaCMC/gel hydrogel formulations. Also, the MN application time duration of 5 min resulted in a highly favorable increase in lidocaine permeation. Furthermore, combining MN and LFS pre-treatments allowed for the time to reach minimum therapeutic lidocaine levels to be significantly reduced. For example, in the case of lidocaine NaCMC/gel, 1:2.66 hydrogel therapeutic thresholds of lidocaine were reached within 7 min of application. The mass transfer effects in which the percentage of lidocaine remained in the full skin depicted the gradual movement of drug in targeting pain receptors below the SC layer. The lidocaine NaCMC/gel 1:2.66 hydrogel treated by MNs and LFS shows a greater mass transfer profile. The US- and MN-treated lidocaine NaCMC/gel 1:2.66 has a 0.18% mass transfer of lidocaine through skin within 2 h compared with 0.01% mass transfer of lidocaine through skin. Therefore, this method is promising and could be of medical use as a painless, easy to administer technique for drug delivery overcoming the time constraints associated with delivery of lidocaine. Lidocaine NaCMC/gel 1:2.66 hydrogel is likely to be the most desirable drug formulation candidate for further developmental studies reaching potentially important pre-clinical and final post clinical stage developments. In order to develop a less polydisperse but low micron scale lidocaine hydrogel formulation requires a longer time frame and added investment. The resources and materials in developing a lidocaine NaCMC/gel

1:2.66 hydrogel without rotary evaporation is economical on a batch scale at present. Lidocaine NaCMC/gel 1:2.33 formulation with defined morphological appearance is able to remain on the surface of the skin for longer durations compared with a lidocaine solution of the same mass loading.

Acknowledgements

The authors acknowledge the help of Craig Chao for his assistance toward the characterization of droplet spreading on skin (Figure 5).

Declaration of interest

The authors report no conflicts of interest. The authors alone are responsible for the content and writing of this article.

References

- Alaie J, Vasheghani-Farahani E, Rahmatpour A, Semsarzadeh MA. (2013). Gelation rheology and water absorption behavior of semi-interpenetrating polymer networks of polyacrylamide and carboxymethyl cellulose. *J Macromolecular Sci, Part B* 52:604–13.
- Al-Qallaf B, Das DB. (2008). Optimization of square microneedle arrays for increasing drug permeability in skin. *Chem Eng Sci* 63: 2523–35.
- Al-Qallaf B, Das DB. (2009). Optimizing microneedle arrays to increase skin permeability for transdermal drug delivery. *Ann New York Acad Sci* 1161:83–94.
- Badran MM, Kuntsche J, Fahr A. (2009). Skin penetration enhancement by microneedle device (DermaRoller®) in vitro: dependency on needle size and applied formulation. *Eur J Pharm Sci* 36:511–23.
- Banks SL, Paudel KS, Brogden NK, et al. (2013). Diclofenac enables prolonged delivery of naltrexone through microneedle-treated skin. *Pharm Res* 28:1211–19.
- Benet LZ, Oie S, Schwartz JB. (1996). Design and optimisation of dosage regimens: pharmacokinetic data. In: Hardman JG, Limbard LE, Molinoff PB, Rudon RW, Gilman AG, eds. *The pharmacological basis of therapeutics*. McGraw Hill: New York, 1707–92.
- Berger J, Reist M, Mayer JM, et al. (2004). Structure and interactions in covalently and ionically crosslinked chitosan hydrogels for biomedical applications. *Euro J Pharm Biopharm* 57:19–34.
- Chao TZ, Trybala A, Starov V, Das DB. (2014). Influence of haematocrit level on the kinetics of blood spreading on thin porous medium during blood spot sampling. *Colloids Surf A: Physicochem Eng Aspects* 451: 38–47.
- Chen B, Wei J, Iliescu C. (2010). Sonophoretic enhanced microneedles array (SEMA) – improving the efficiency of transdermal drug delivery. *Sens Actuators B: Chem* 145:54–60.
- Cheung K, Han T, Das DB. (2014). Effect of force of microneedle insertion on the permeability of insulin in skin. *J Diabetes Sci Technol* 8:444–52.
- Chow KT, Chan LW, Heng PWS. (2008). Characterization of spreadability of nonaqueous ethylcellulose gel matrices using dynamic contact angle. *J Pharm Sci* 97:3467–81.
- De Boer AG, Breimer DD, Mattie H, et al. (1979). Rectal bioavailability of lidocaine in man: partial avoidance of “first-pass” metabolism. *Clin Pharmacol Ther* 26:701–9.
- Ducel V, Richard J, Saulnier P, et al. (2004). Evidence and characterization of complex coacervates containing plant proteins: application to the microencapsulation of oil droplets. *Colloids Surf A* 232:239–47.
- Ebrahimi S, Abbasnia K, Motealleh A, et al. (2012). Effect of lidocaine phonophoresis on sensory blockade: pulsed or continuous mode of therapeutic ultrasound? *Physiotherapy* 98:57–63.
- Fasinu P, Viness PV, Ndesendo VMK, et al. (2011). Diverse approaches for the enhancement of oral drug bioavailability. *Biopharm Drug Dispos* 32:185–209.
- Fen-Lin W, Razzaghi A, Souney PF. (1993). Seizure after lidocaine for bronchoscopy: case report and review of the use of lidocaine in airway anesthesia. *Pharmacotherapy* 13:72–8.
- Gill HS, Prausnitz MR. (2007). Coated microneedles for transdermal delivery. *J Controlled Release* 117:227–37.
- Giudice EL, Campbell JD. (2006). Needle-free vaccine delivery. *Adv Drug Deliv Rev* 58:68–89.
- Ghosh P, Brogden NK, Stinchcomb AL. (2013a). Effect of formulation pH on transport of naltrexone species and pore closure in microneedle-enhanced transdermal drug delivery. *Mol Pharm* 10: 2331–9.
- Ghosh P, Pinninti RR, Hammell DC, et al. (2013b). Development of a codrug approach for sustained drug delivery across microneedle-treated skin. *J Pharm Sci* 102:1458–67.
- Grossman JI, Cooper JA, Frieden IJ. (1969). Cardiovascular effects of infusion of lidocaine on patients with heart disease. *Am J Cardiol* 24: 191–7.
- Guo L, Qiu Y, Chen J, et al. (2013). Effective transcutaneous immunization against hepatitis B virus by a combined approach of hydrogel patch formulation and microneedle arrays. *Biomed Microdevices* 15:1077–85.
- Gupta KC, Ravi Kumar MNV. (2000). Semi-interpenetrating polymer network beads of crosslinked chitosan–glycine for controlled release of chlorpheniramine maleate. *J Appl Polym Sci* 76:672–83.
- Han T, Das DB. (2013). Permeability enhancement for transdermal delivery of large molecule using low frequency sonophoresis combined with microneedles. *J Pharm Sci* 102:3614–22.
- Hedge NR, Kaveri SV, Bayry J. (2011). Recent advances in the administration of vaccines for infectious diseases: microneedles as painless delivery devices for mass vaccination. *Drug Discovery Today* 16:1061–8.
- Herwadkar A, Sachdeva V, Taylor LF, et al. (2012). Low frequency sonophoresis mediated transdermal and intradermal delivery of ketoprofen. *Int J Pharm* 423:289–96.
- Huet PM, Leloirier J. (1980). Effects of smoking and chronic hepatitis B on lidocaine and indocyanine green kinetics. *Clin Pharmacol Ther* 28: 208–15.
- Igaki M, Higashi T, Hamamoto S, et al. (2013). A study of the behavior and mechanism of thermal conduction in the skin under moist and dry heat conditions. *Skin Res Technol* 20:43–9.
- Ito Y, Ohta J, Imada K, et al. (2013). Dissolving microneedles to obtain rapid local anesthetic effect of lidocaine at skin tissue. *J Drug Targeting* 21:770–5.
- Kim Y, Park J, Prausnitz MR. (2012). Microneedles for drug and vaccine delivery. *Adv Drug Deliv Rev* 64:1547–68.
- Kochhar JS, Lim WXS, Zou S, et al. (2013). Microneedle integrated transdermal patch for fast onset and sustained delivery of lidocaine. *Mol Pharm* 10:4272–80.
- Kwon SY. (2004). In vitro evaluation of transdermal drug delivery by a micro-needle patch. *Controlled Release Society 31st Annual Meeting Transactions*. Honolulu, Hawaii. Available from: http://www.theraject.com/news_events/Abstract_2004CRS.pdf
- Li X, Zhao R, Qin Z, et al. (2010). Microneedle pretreatment improves efficacy of cutaneous topical anesthesia. *Am J Emergency Med* 28: 130–4.
- Li XG, Zhao RS, Qin ZL, et al. (2008). Painless microneedle transdermal patch enhances permeability of topically applied lidocaine. *Chinese J New Drugs* 17:597–601.
- Merino G, Kalia YN, Delgado-Charro MB, et al. (2003). Frequency and thermal effects on the enhancement of transdermal transport by sonophoresis. *J Controlled Release* 88:85–94.
- Milewski M, Stinchcomb A. (2011). Vehicle composition influence on the microneedle-enhanced transdermal flux of naltrexone hydrochloride. *Pharm Res* 28:124–34.
- Nayak A, Das DB. (2013). Potential of biodegradable microneedles as a transdermal delivery vehicle for lidocaine. *Biotechnol Lett* 35: 1351–63.
- Nayak A, Das DB, Vladislavjević GT. (2014). Microneedle assisted permeation of lidocaine carboxymethylcellulose with gelatine co-polymer hydrogel. *Pharm Res* 31:1170–84.
- Olatunji O, Das DB, Nassehi V. (2012). Modelling transdermal drug delivery using microneedles: effect of geometry on drug transport behaviour. *J Pharm Sci* 101:164–75.
- Olatunji O, Das DB, Garland MJ, et al. (2013). Influence of array interspacing on the force required for successful microneedle skin penetration: theoretical and practical approaches. *J Pharm Sci* 102: 1209–21.
- Olatunji O, Igwe CC, Ahmed AS, et al. (2014). Microneedles from fish scale biopolymer. *J Appl Polym Sci* 131:1–10. DOI: 10.1002/app.40377.

- Park N, Kwon B, Kim IS, Cho J. (2005). Biofouling potential of various NF membranes with respect to bacteria and their soluble microbial products (SMP): characterizations, flux decline, and transport parameters. *J Membr Sci* 258:43–54.
- Polat B, Hart D, Langer R, Blankschtein D. (2011). Ultrasound-mediated transdermal drug delivery: mechanisms, scope, and emerging trends. *J Controlled Release* 152:330–48.
- Roxhed N, Gasser TC, Griss P. (2007). Penetration-enhanced ultrasharp microneedles and prediction on skin interaction for efficient transdermal drug delivery. *J Microelectromech Syst* 16:1429–40.
- Scarfone RJ, Jasani M, Gracely EJ. (1998). Pain of Local Anesthetics: rate of administration and buffering. *Ann Emergency Med* 31:36–40.
- Schulz M, Iwersen-Bergmann S, Andresen H, Schmoldt A. (2012). Therapeutic and toxic blood concentrations of nearly 1,000 drugs and other xenobiotics. *Crit Care* 16:R136.
- Sekkat N, Kalia YN, Guy RH. (2004). Porcine ear skin as a model for the assessment of transdermal drug delivery to premature neonates. *Pharm Res* 21:1390–7.
- Shah UU, Roberts M, Orlu GM, et al. (2011). Needle-free and microneedle drug delivery in children: a case for disease-modifying antirheumatic drugs (DMARDs). *Int J Pharm* 416:1–11.
- Shipton EA. (2012). Advances in delivery systems and routes for local anaesthetics. *Trends Anaesth Critic Care* 2:228–33.
- Sintov AC, Shapiro L. (2004). New microemulsion vehicle facilitates percutaneous penetration in vitro and cutaneous drug bioavailability in vivo. *J Controlled Release* 95:173–83.
- Sze A, Erickson D, Ren L, Li D. (2003). Zeta-potential measurement using the Smoluchowski equation and the slope of the current-time relationship in electroosmotic flow. *J Colloid Interface Sci* 261:402–10.
- Wilson JR, Kehl LJ, Beiraghi S. (2008). Enhanced topical anesthesia of 4% lidocaine with microneedle pretreatment and iontophoresis. *Northwest Dentistry* 87:40–1.
- Wolloch L, Kost J. (2010). The importance of microjet vs shock wave formation in sonophoresis. *J Controlled Release* 148:204–11.
- Xu R, Wu C, Xu H. (2007). Particle size and zeta potential of carbon black in liquid media. *Carbon* 45:2806–9.
- Zhang Y, Brown K, Siebenaler K, et al. (2012a). Development of lidocaine-coated microneedle product for rapid, safe, and prolonged local analgesic action. *Pharm Res* 29:170–7.
- Zhang Y, Siebenaler K, Brown K, et al. (2012b). Adjuvants to prolong the local anesthetic effects of coated microneedle products. *Int J Pharm* 439:187–92.
- Zhang D, Das DB, Rielly CD. (in press). Potential of microneedle-assisted micro-particle delivery by gene guns: a review. *Drug Delivery*. DOI: 10.3109/10717544.2013.864345.